

"The Magnetized Interstellar Medium"
 8–12 September 2003, Antalya, Turkey
 Eds.: B. Uyaniker, W. Reich & R. Wielebinski

The DRAO 26-m Large Scale Polarization Survey at 1.41 GHz

M. Wolleben^{1,2}, T.L. Landecker², W. Reich¹ and R. Wielebinski¹

¹Max-Planck-Institut für Radioastronomie, Auf dem Hügel 69, 53121 Bonn, Germany

²Dominion Radio Astrophysical Observatory, Herzberg Institute of Astrophysics, National Research Council of Canada, Box 248, Penticton, BC V2A 6J9, Canada

Abstract. The Effelsberg telescope as well as the DRAO synthesis telescope are currently surveying the Galactic polarized emission at $\lambda 21$ cm in detail. These new surveys reveal an unexpected richness of small-scale structures in the polarized sky. However, observations made with synthesis or single-dish telescopes are not on absolute intensity scales and therefore lack information about the large-scale distribution of polarized emission to a different degree. Until now, absolutely calibrated polarization data from the Leiden/Dwingeloo polarization surveys are used to recover the missing spatial information. However, these surveys cannot meet the requirements of the recent survey projects regarding sampling and noise and new polarization observation were initiated to complement the Leiden/Dwingeloo Survey. In this paper we will outline the observation and report on the progress for a new polarization survey of the northern sky with the 26-m telescope of the DRAO.

1 Motivation

Over the past several years a number of survey projects were launched in order to map the polarized emission from the Galaxy in great detail (e.g. Junkes et al. 1987, Duncan et al. 1997, Uyaniker et al. 1998, Taylor et al. 2003). Single-dish as well as synthesis telescopes located in the northern and southern hemisphere are being used. However, observations made with synthesis telescopes are systematically affected by a missing zero spacing problem, which prevents the detection of extended emission. In a similar way, single-dish observations can lack a large-scale emission component, which is often lost during the data reduction process when attempts are made to subtract the ground radiation from the observations. If the ground radiation is not known exactly, one cannot distinguish between real sky signal and radiation from the ground.

For an interpretation of polarimetric observations, an accurate absolute calibration is essential. Other than for total power observations, absolute calibration of polarization data means to calibrate vectorial quantities. Surprisingly on first sight, this means that absolute calibration of polarized intensity maps can turn emission-type objects into minima in PI, and vice versa. Also rotation measures can be affected by an inaccurate calibration of polarization data.

Missing zero spacings in interferometric observations are added from single-dish observations. In turn, large-scale components in single-dish data are recovered by using existing absolutely calibrated polarization data from the 60's and 70's made with single-dish telescopes, e.g. the Leiden/Dwingeloo polarization surveys (Brouw & Spoelstra 1976). However, the severe under-sampling and relatively high noise of these data often makes an accurate calibration of the recent surveys impossible. Until now, these absolutely calibrated data from the Leiden/Dwingeloo surveys laid the foundation for the calibration chain up to the synthesis telescopes, and therefore an improvement of these *old* data regarding sampling and noise became necessary.

2 The DRAO 26-m Telescope and Receiver

The 26-m telescope at DRAO is on an equatorial mount, with a mesh surface and the receiver placed in its prime focus on three feed-legs. The pointing accuracy is about $48''$. The receiver used for polarimetric observations consists of a quadrature HF-hybrid which forms circular out of linear polarization,

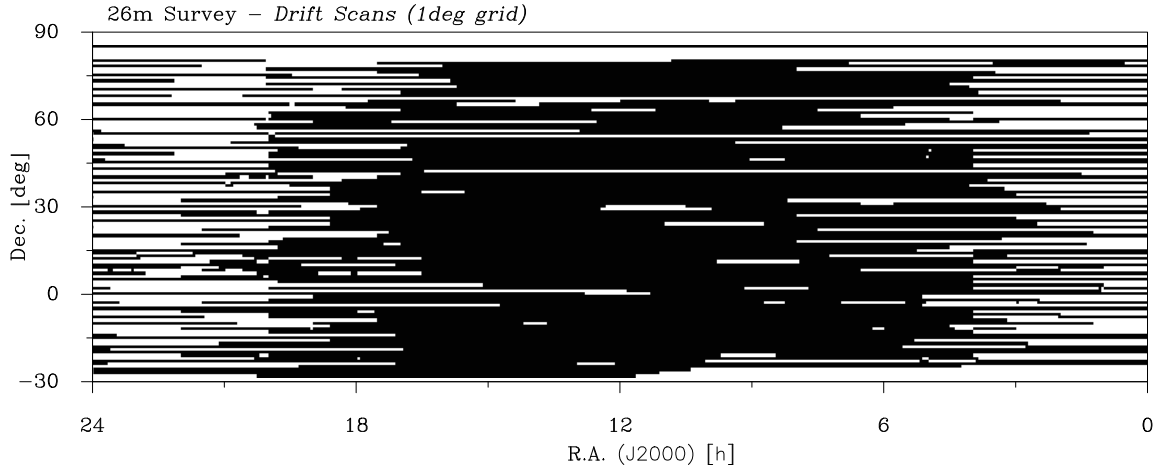


Fig. 1. Map showing the sky coverage of the new survey. Black lines indicate drift scans.

two uncooled FET-amplifiers for both hands of polarization operating on room temperature, and circulators to improve matching. The system temperature was about 150 K. Two HF-bandpass filters and additional IF-filters were used to limit the bandwidth to 12 MHz (10 MHz for data obtained in November 2002). An integrated noise source was used to inject a calibration signal every 32 seconds for a duration of 400 ms into the X and Y part of the receiving system. Gain variations were less than 4% over a period of 40 days.

The IF-polarimeter is an analog 2-channel multiplier providing the four correlation products RR, LL, RL, and LR. The polarimeter was brought from the MPIfR, Bonn and is of the type used on the Effelsberg telescope. It operates at an IF of 150 MHz and a total bandwidth of 50 MHz. Every 4 seconds, an internal phase shifter was switched to invert the signs of the two cross-correlation products. This was necessary to correct for any electronic drifts in the polarimeter. Data were integrated and recorded every 40 ms.

3 Observation, Calibration and Reduction Steps

Observations were made during seven months from November 2002 through May 2003 using the 26-m telescope in the drift-scan mode. Each night one declination was observed. We made 168 drift scans covering the entire sky observable from the DRAO with the telescope stationary on the meridian. Many regions could be observed with a 1° separation in declination or smaller; some could only be observed with a 5° sampling in declination. Along right ascension the drift scans are fully sampled. The center frequency of the receiver was tuned to 1410 MHz, avoiding the H α line emission. Most of the observations were done during the night. Prior and after each drift scan, standard calibration sources were mapped.

The hybrid introduces cross-talk and extensive calibration was needed to transform the four polarimeter output channels into true Stokes parameters. The following steps were applied to the raw data:

Flagging: Interference removal was done automatically by a flagging algorithm which searches for short-term peaks which are $4.5\sigma_{\text{rms}}$ above the average signal level over a 2 minute time window.

Pre-scaling and rotation: The vector formed out of the four correlation products RR, LL, RL, and LR is multiplied with a 4×4 -matrix, similar to a Müller matrix with the difference that

correlation products instead of Stokes parameters are transformed. This reduction step includes a pre-scaling and rotation in order to transform the arbitrary polarimeter units into meaningful temperatures in the equatorial system. An iterative method is used to find the appropriate correction matrix. This algorithm starts with the unit matrix and successively modifies matrix entries until the best-fit matrix is found. The quality of the matrix can be estimated by the correlation of the corrected raw data with the absolutely calibrated Leiden/Dwingeloo polarization data, resp. the Stockert total-power data (Reich 1982, Reich & Reich 1986).

Gain and phase: Electronic gain and phase variations in the receiving system were recorded by changes in the signal level of the calibration signal in all four channels. The standard temperature and position angle of the calibration signal assumed for this survey is given by the average values over the seven months.

Ground radiation: Spurious polarization is picked up by the side-lobes of the telescope. This mainly ground-based signal can be intrinsically unpolarized, however, the side-lobes are highly polarized, which results in an elevation- and azimuth-dependent polarization component. Since we exclusively observed in the meridian we only have to deal with the elevation dependency. For the purpose of deriving a ground-radiation model we made elevation scans along the meridian at different sidereal times. Their average served as a time-independent model (see Fig. 2) which was used to subtract the ground-radiation component.

Sun and ionospheric Faraday rotation: Beside the rather stable ground radiation, which was modelled, the sun is another strong source of spurious polarization. In the same way as the ground is detected as a polarized signal, the bright signal from the sun also causes strong polarized signals if radiating into the side-lobes. Therefore observations were limited to night-time to circumvent interference from the sun. In addition, ionospheric Faraday rotation can affect the position angle of polarized signals. This effect is negligible during the night. Whenever day-time data were used, we cross-checked the data against neighboring drift scans for possible sun interference or ionospheric Faraday rotation.

De-striping: Although the receiving system is fairly stable, there are remaining variations in the system temperature. We believe that these variations are caused by seasonal changes of the ground radiation or temperature drifts in the front-end part of the receiver. Changing offsets in the system temperature show up as stripes in the final map and we compared in an iterative method each drift scan with its neighboring scans to correct for variations in the system temperature.

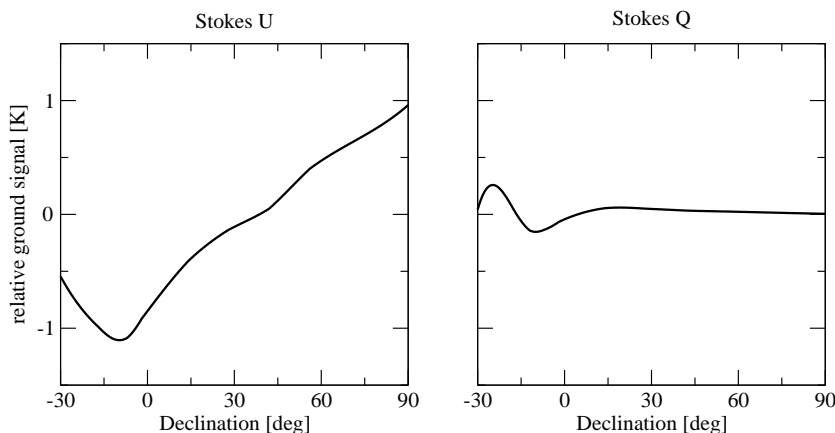


Fig. 2. Ground radiation profiles for Stokes U and Q derived by averaging elevation scans.

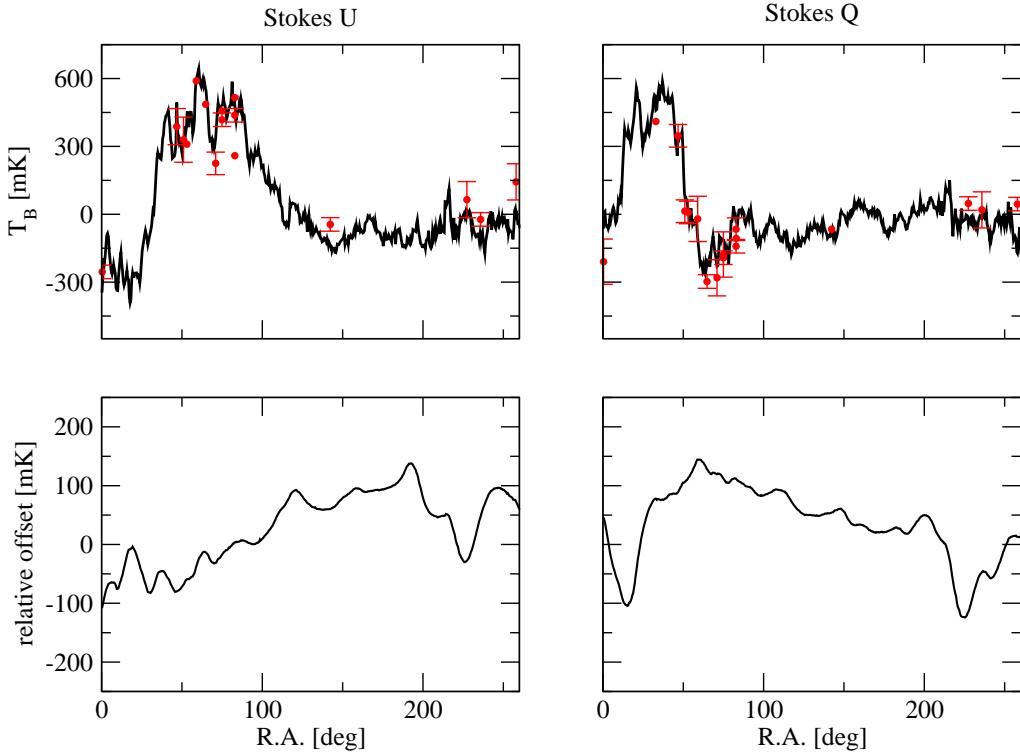


Fig. 3. Drift scan at 56° declination. The upper panels show Stokes U and Q brightness temperatures. Available data points from the Leiden/Dwingeloo survey are overlaid with error bars indicating the quoted errors. The lower panels show the relative system temperature derived from the de-striping algorithm.

Final scaling, rotation, and instrumental polarization: After applying the reduction steps discussed above, a second pass Müller matrix fit was necessary to improve the correlation with the reference values from the Leiden/Dwingeloo survey. Also the cross-talk introduced by the receiver was now corrected.

The digitized version of the Leiden/Dwingeloo data at 1.4 GHz provides Stokes U and Q brightness temperatures for more than 1600 different positions on the sky. About 700 positions are covered by our survey within a radius of $15'$. These common data points serve as reference values for the matrix fits discussed above. This means that our temperature scale fully relies on the Leiden/Dwingeloo data.

4 Example Drift Scan

In Fig. 3 we show an example drift scan at 56° declination. The drift scan passes the *fan*-region, a bright, polarized region centered at about $\alpha = 50^\circ$, $\beta = 65^\circ$. Considering the mean errors (60 mK as quoted for the Leiden/Dwingeloo data, and about 30 mK for the new survey), the Stokes U and Q distributions of both surveys are in good agreement for this drift scan. Remarkable is the appearance of small-scale structure which cannot be seen in the Leiden/Dwingeloo data set because of its coarse sampling. Fig. 3 also shows the offsets in Stokes U and Q , which apparently suffer from a temperature drift. This offset drift is most likely caused by variations of the receiver temperature or local environmental conditions and was derived from the de-striping algorithm.

5 Repeatability of Drift Scans

Repeatability of drift scans is an important criterion for accuracy. In Fig. 4 (top panels) we display two drift scans observed at the same declination ($\delta = 40^\circ$). The repetition scan was observed 10 weeks

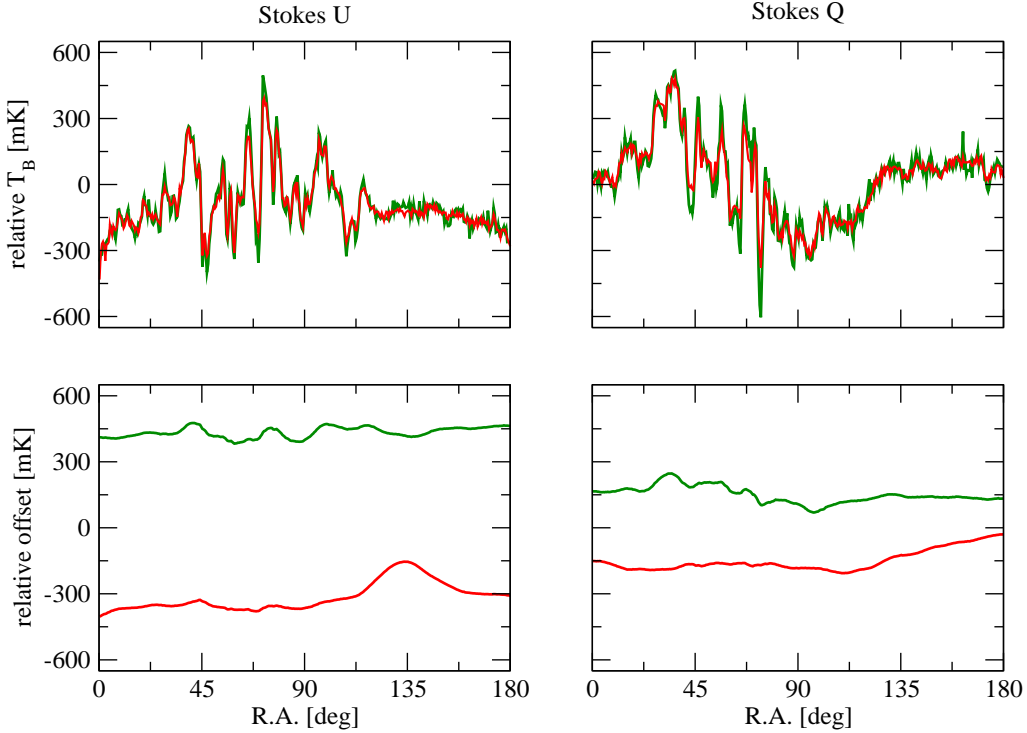


Fig. 4. Two drift scans at 40° declination observed on Nov. 20 (green) and Jan. 28, 2002 (red). The upper panels show brightness temperatures for Stokes U and Q . In the lower panels the relative system temperature is plotted.

later. Variations in the system temperature have been corrected as described above and are shown in the bottom panels of Fig. 4. Stokes U and Q values of both drift scans are in good agreement. The systematic difference in the relative offsets is caused by a change in the bandwidth of the IF-filters, and, as a result, the noise in all later drift scans decreased.

6 Correlation of the DRAO and Leiden/Dwingeloo Polarization Survey

In the previous section a comparison of both surveys is made for a single scan at 56° declination. But how do the entire data sets compare? In Fig. 5 the correlation of polarized intensities is shown for all positions which are common to both surveys. Beside the linear correlation, a large scatter of polarized intensities is visible. The correlation coefficients for Stokes U and Q vary between 0.85 and 0.87 for this preliminary set of data. With an average error in the Leiden/Dwingeloo data of 60 mK, the error in our data thus results to about 30 mK.

7 Preliminary Map of Polarized Intensity

In Fig. 6 we show a preliminary map of the polarized intensity calculated by $PI = \sqrt{U^2 + Q^2}$. The Stokes U and Q data have been convolved to match a beam size of 4° . Two bright polarized regions of the northern sky are sticking out: the *fan*-region, and the north polar spur at $\alpha = 230^\circ$, $\delta = 18^\circ$. It is planned to continue the observations to complete the sampling.

References

Brouw W. N., Spoelstra, T. A. T. (1976) *Astron. Astrophys. Suppl.* **26**, 129.
 Duncan A. R., Haynes R. F., Jones K. L., Stewart R. T. (1997) *Mon. Not. R. Astron. Soc.* **291**, 279.
 Junkes N., Fürst E., Reich W. (1987) *Astron. Astrophys. Suppl.* **69**, 451.

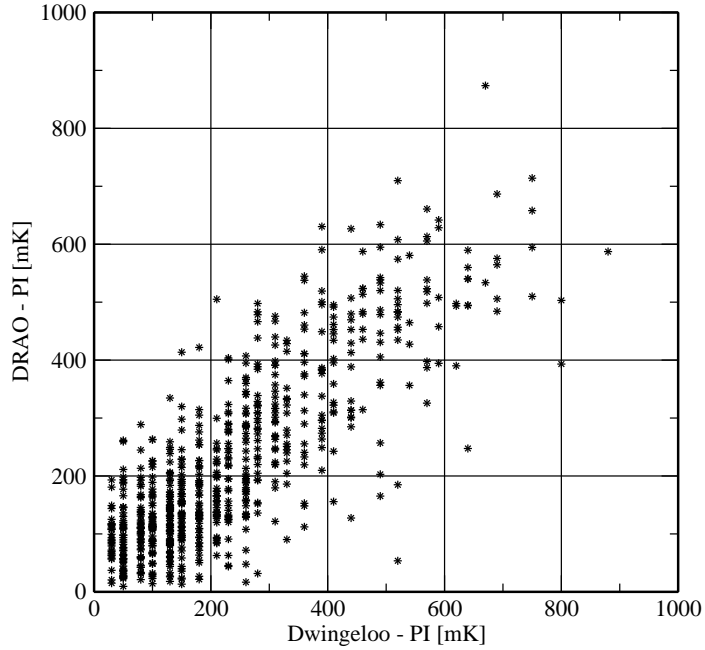


Fig. 5. Comparison of polarized intensities of the DRAO and Leiden/Dwingeloo polarization surveys.

Reich W. (1982) *Astron. Astrophys. Suppl.* **48**, 210.
 Reich P., Reich W. (1986) *Astron. Astrophys. Suppl.* **63**, 205.
 Taylor A. R. et al. (2003) *Astron. J.* **125**, 3145.
 Uyaniker B. et al. (1998) *Astron. Astrophys. Suppl.* **132**, 401.

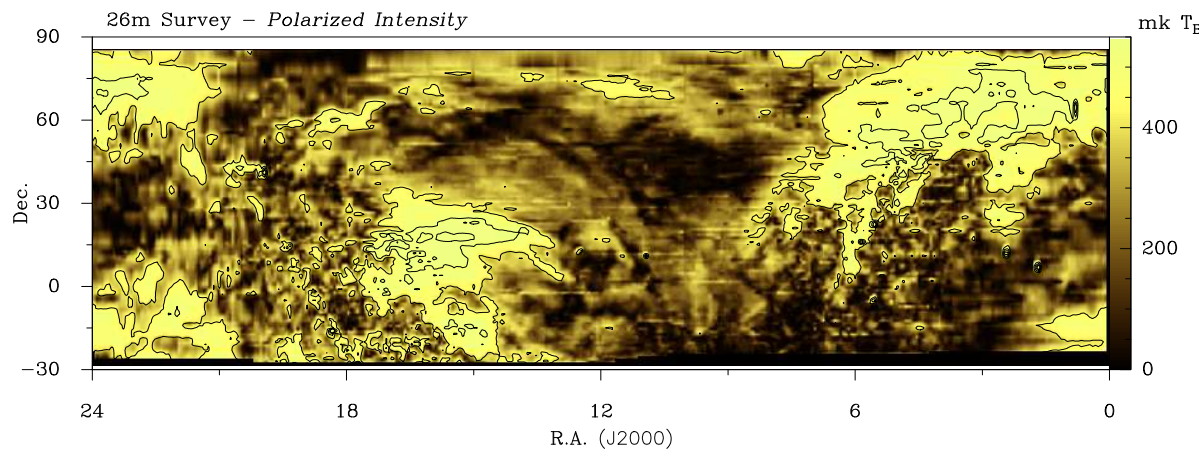


Fig. 6. Preliminary map of the polarized intensity. The original data have been convolved to match a beam size of 2° .